Wire edge dependent magnetic domain wall creep

Wire edge dependent magnetic domain wall creep

L. Herrera Diez,[1,*] V. Jeudy,[2] G. Durin,[3] A. Casiraghi,[3] Y. T. Liu,[1] M. Voto,[4] G. Agnus,[1] D. Bouville,[1] L. Vila,[5] J. Langer,[6] B. Ocker,[6] L. Lopez-Diaz,[4] and D. Ravelosona[1]

[1]*Centre de Nanosciences et de Nanotechnologies, CNRS, Univ. Paris-Sud, Université Paris-Saclay, C2N Orsay, 91405 Orsay Cedex, France*
[2]*Laboratoire de Physique des Solides, CNRS, Univ. Paris-Sud, Université Paris-Saclay, 91405 Orsay Cedex, France*
[3]*Istituto Nazionale di Ricerca Metrologica, Strada delle Cacce 91, 10135 Torino, Italy*
[4]*Departamento de Física Aplicada, Universidad de Salamanca, Plaza de la Merced s/n. 37008 Salamanca, Spain*
[5]*Univ. Grenoble Alpes, CEA, CNRS, Grenoble INP, INAC-Spintec, 38000 Grenoble, France*
[6]*Singulus Technology AG, Hanauer Landstrasse 103, 63796 Kahl am Main, Germany*

(Received 6 December 2017; revised manuscript received 2 July 2018; published 17 August 2018)

While edge pinning is known to play an important role in sub-μm wires, we demonstrate that strong deviations from the universal creep law can occur in 1 to 20 μm wide wires. Magnetic imaging shows that edge pinning translates into a marked bending of domain walls at low drive and is found to depend on the wire fabrication process and aging. Edge pinning introduces a reduction of domain wall velocity with respect to full films which increasingly dominates the creep dynamics as the wire width decreases. We show that the deviations from the creep law can be described by a simple model including a counter magnetic field which links the width of the wire to the edge dependent pinning strength. This counter field defines a key nonuniversal contribution to creep motion in patterned structures.

DOI: 10.1103/PhysRevB.98.054417

In the limit of low driving forces magnetic domain walls (DW) provide an interesting model for the study of the motion of elastic interfaces in a random disorder potential [1–5]. DWs driven by feeble forces move in a thermally activated regime and strongly interact with defects, showing a jagged DW profile highlighting the presence of pinning. This universal behavior describes a wide variety of systems such as the dynamics of vortices in superconductors [6], propagation of liquid wetting lines on surfaces [7], and crack formation in solids [8].

In this slow dynamic regime, the velocity obeys an Arrhenius law $v \sim e^{-\Delta E/(k_B T)}$ (k_B being the Boltzmann constant and $k_B T$ the thermal activation energy) where the effective pinning energy barrier presents a power law divergence $\Delta E \sim f^{-\mu}$ when the driving force f is close to zero drive ($f \to 0$). μ is the so-called creep exponent reflecting the competition between elastic and pinning interactions; it depends on the dimensionality of the system and on the range of interactions. DW motion in a thin film with a weak pinning potential [2] is generally compatible with theoretical predictions [1] describing the motion of a one-dimensional (1D) elastic line in a two-dimensional medium. In this framework, the dynamics is ruled by the critical exponent $\mu = 1/4$.

Recently, an ultimate general description of creep DW velocity (v) was extended up to the depinning threshold [9]. An empirical universal energy barrier function was proposed to describe creep motion as a function of the reduced driving force H/H_{dep}:

$$v(H,T) = v(H_{\mathrm{dep}},T) exp^{-\Delta E/k_B T} \tag{1}$$

$$\Delta E = k_B T_{\mathrm{dep}} \left[\left(\frac{H}{H_{\mathrm{dep}}} \right)^{-\mu} - 1 \right], \tag{2}$$

where H_{dep} is the depinning threshold at which the effective pinning energy barrier vanishes ($\Delta E \to 0$) and $k_B T_{\mathrm{dep}}$ is a characteristic pinning energy scale. In a variety of thin films with ferromagnetic and ferrimagnetic properties, amorphous and crystalline structures, metallic and semiconducting properties, the dynamic response agrees with the empirical description in Eqs. (1) and (2).

In narrow wires, edge roughness can have a large impact on domain wall creep dynamics. While still adjusting to the creep model ruled by $\mu = 1/4$, DW velocity in Pt/Co/Pt micro- and nanowires [3] can be critically reduced by wire edge roughness. In other materials, changes in the universality class of the system can occur due to changes in dimensionality [10], the nature of disorder, or the driving force [11,12], but show no evidence of edge related distortions or its possible contribution to the universal behavior is not taken into account.

In this study we show that edge roughness can induce important deviations from the creep model in Ta/CoFeB/MgO wires with dimensions orders of magnitude larger than those required for a dimensionality transition (1D to 0D DW) [10]. DW creep velocity in full films and 200 μm wires can be well described by Eqs. (1) and (2), however, lower velocities than those predicted by the creep model are observed as the wire width and driving force decrease. These deviations are also shown to be strongly linked to the fabrication process of the

*liza.herrera-diez@c2n.upsaclay.fr

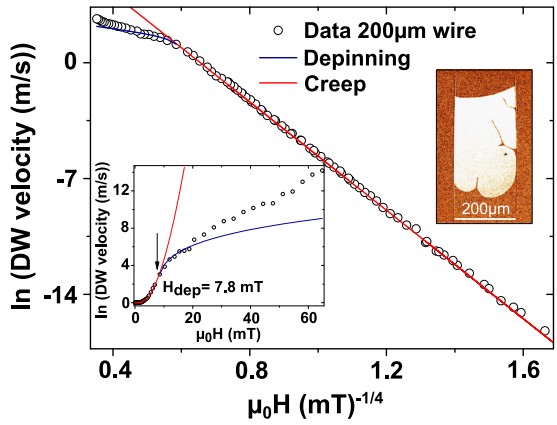

FIG. 1. ln(DW velocity) vs $\mu_0 H^{-1/4}$ in a 200 μm wire. The insets show (left) the same plot in a linear scale highlighting the position of H_{dep} and (right) the DW profile at low drive (0.33 mT $\approx H_{dep}/24$).

wires and aging in a series of 20 μm wide wires. To describe the strong influence of edge pinning in the creep dynamics we propose a model where edge pinning is accounted for by a counter field acting on the DW. Alternative models assuming a variation of the critical creep exponent are also discussed.

The samples investigated are Si/SiO_2/Ta (5 nm)/$Co_{20}Fe_{60}B_{20}$ (1 nm)/MgO (2 nm)/Ta (3 nm) films annealed at 300 °C exhibiting perpendicular magnetic anisotropy. Optical lithography was used to produce arrays of microwires of 1 μm, 5 μm, 10 μm, 20 μm, 50 μm, 100 μm, and 200 μm. In all cases magnetic DW motion was measured by differential Kerr microscopy under magnetic fields applied perpendicular to the sample plane. Figure 1 shows the good correspondence between the creep model and the DW dynamics in a 200 μm wide wire [the red line is the fitting to Eq. (1)]. This is also the case in the unpatterned CoFeB pristine films and in equivalent films exposed to He^+ ion irradiation [13] where magnetic anisotropy and defect densities are modulated. The inset (left) shows the position of H_{dep}, which we define to be the intersection between the fitting lines corresponding to the creep and depinning models [14]. The typical DW creep profile found in unpatterned films is also observed in 200 μm wide wires [Fig. 1, inset (right)] where a number of strong pinning sites hinders DW propagation at low drive (0.33mT $\approx H_{dep}/24$). Very rough DW profiles are less commonly found in high quality CoFeB/MgO materials given the low defect density with respect to other magnetic systems [15]. The DW profile observed in 200 μm wires combined with a good agreement with the creep model indicates that wires of these dimensions are not greatly affected by edge pinning and still show the same DW dynamics as the full film. Therefore, the dynamics in 200 μm wires is taken from here on as the reference for the creep model dynamics in this system.

Figure 2 shows the DW velocity curves of wires of different widths ranging from 100 to 1 μm which are seen to progressively deviate from the creep model at low drive as the wire width is reduced. Nevertheless, all wires have the tendency to recover the creep model dynamics as the magnetic field increases. Figure 3(a) shows similar deviations induced by the structure of the wire edges and aging in a 20 μm wide wire series. Wire A is the 20 μm structure presented in Fig. 2 while wires B and C were fabricated with different lithography and etching parameters with respect to wire A. The difference between wires B and C is aging: Wire C has been on a shelf for more than two years while wire B was measured right after fabrication, just like wire A. In these three cases the wire edges

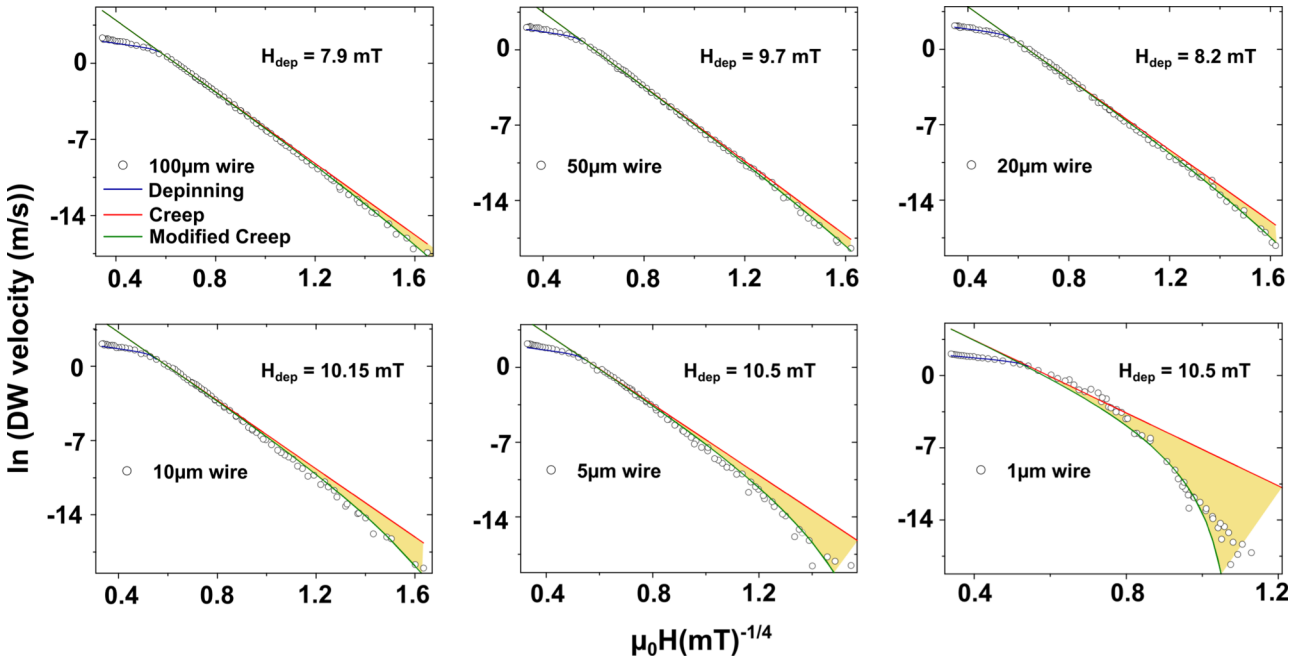

FIG. 2. ln(DW velocity) vs $\mu_0 H^{-1/4}$ for different wire widths. Deviations from the creep model ($\mu = 1/4$) are observed as the wire width and driving field decrease. In the high field region the fitting line corresponds to the depinning model; at low drive a modified creep model including a counter field is also plotted.

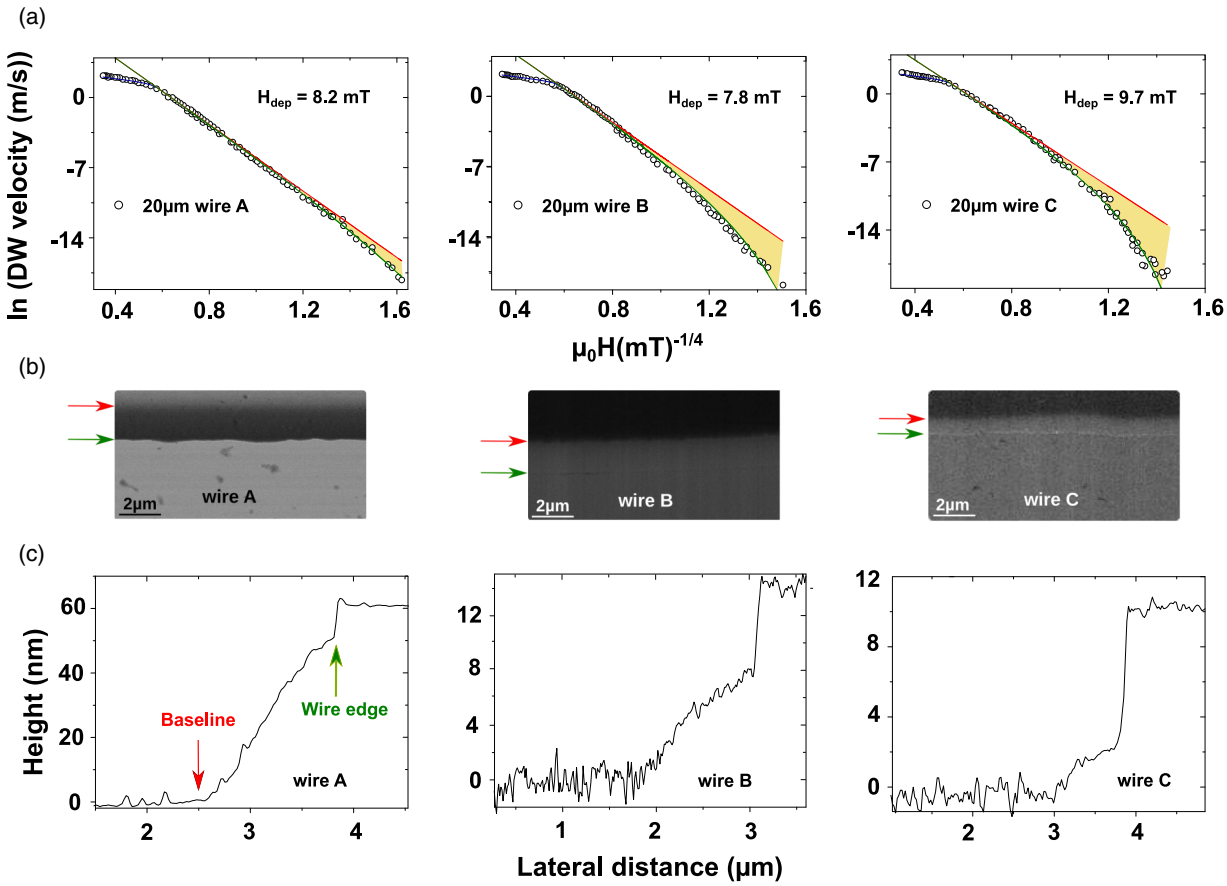

FIG. 3. (a) ln(DW velocity) vs $\mu_0 H^{-1/4}$ for different 20 μm wire series. The magnitude of the deviation depends on the different fabrication processes (A and B) and aging (C). Note that wire A belongs to the variable width series presented in Fig. 2. (b) SEM images and (c) AFM scans of each wire presented in (a).

do not show significant discrepancies in terms of roughness, found to be on average in the 200 nm range as can be seen in the SEM (scanning electron microscopy) images presented in Fig. 3(b). However, edge profiles have a smaller 'tail' (the region between the baseline and the wire edge) for wires B and C, fabricated with the same lithography and etching process as shown by the AFM (atomic force microscopy) scans presented in Fig. 3(c). The effect of aging does not show prominently as a structural feature and is thought to be related to oxidation effects. This shows the impact of small variations, not necessarily related to prominent topography features, of the quality of the wire edges on the edge pinning potential.

Figure 4(a) presents the DW profile after motion under constant magnetic fields near $H_{\mathrm{dep}}/20$ for wires A, B, and C ($H_{\mathrm{dep}} = 8.2$ mT, 7.8 mT, 9.7 mT for wires A, B, and C, respectively). A significant rounding of the DW front is evidenced for wire C while a less pronounced effect is seen for wire B. An even more reduced signature is visible in wire A indicating that the degree of bending of the DW front is likely to be correlated with the magnitude of the deviations from the creep model, supporting the idea that it is an edge pinning driven effect. In this case the DW profile seems to be predominantly affected by edge pinning in contrast to that in Fig. 1 (inset, 200 μm wire) where the large width of the wire allows for the DW to find several intrinsic pinning sites along its path. The comparison with Fig. 1 also suggests that the critical width of around 20 μm, where deviations start to increase dramatically, is also a length scale similar to the distribution of strong pinning sites in the unpatterned material. Therefore, the onset of the critical variations in the creep dynamics could be correlated with this length scale. It is to be noted that the

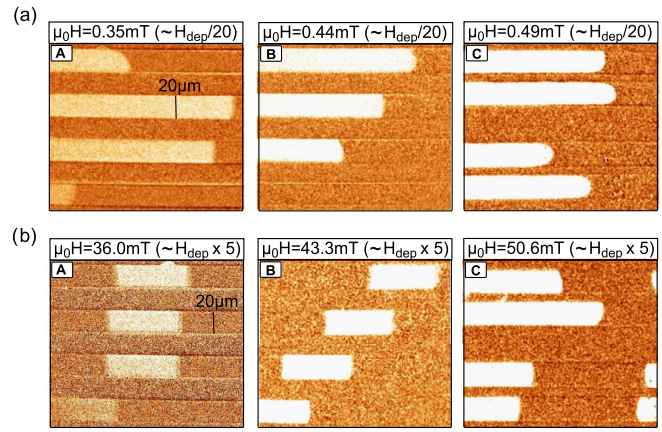

FIG. 4. Wires A, B, and C showing DW displacements under $H_{\mathrm{dep}}/20$ (a) and $H_{\mathrm{dep}} * 5$ (b). The DW curvature seen in the creep regime is highly suppressed beyond H_{dep}.

curvature of the DWs in the creep regime is largely suppressed in the flow regime, as shown in Fig. 4(b), for applied fields of nearly $H_{dep} * 5$. This indicates that the strong modification seen in the DW profile is indeed an effect of the creep dynamics that is consequently suppressed for DW motion at fields beyond H_{dep}.

I. COUNTER FIELD MODEL

This reduction of DW velocity due to edge pinning at low drive can be thought of as the contribution of a field H_{edge} acting against the external driving magnetic field H. In consequence, the DW velocity in the presence of edge pinning would be expected to be lower for the same applied field H. In terms of the creep model presented earlier, the expression for the universal energy barrier ΔE [Eq. (2)] can be modified in order to include the contribution of a counter field H_{edge} as follows:

$$\Delta E = k_B T_{dep}\left[\left(\frac{H - H_{edge}}{H_{dep}}\right)^{-\mu} - 1\right]. \quad (3)$$

The fitting lines of the DW velocity curves with this modified creep model are shown in Fig. 2 for the variable width wire series and in Fig. 3(a) for the 20 μm wire series. These curves show that the counter field model proposed describes much more accurately the DW dynamics in the presence of edge pinning than the pure bulk creep model. It is worth noting that a similar expression has already been proposed to describe the 'retardation' of DW motion in the presence of an inhomogeneous dipolar stray field [16].

Further insight into the physics of H_{edge} can be extracted by proposing a simplified model. In the absence of edge pinning (H_{edge}= 0), bulk pinning dominates the system and defines the energy needed to move a DW over a distance Δx [see Fig. 5(a)], which involves switching a volume equal to $v = \Delta x t w$, where t and w are the thickness and width of the wire, respectively. This energy is provided by the applied magnetic field and has the form $2M_s H \Delta x t w$. For the depinning condition to be fulfilled, in compliance with Eq. (2), it is necessary that $H = H_{dep}$. In this scenario we also consider that the DW surface tension σ, parallel to the DW and with opposite directions at the wire edges [see Fig. 5(a)], keeps the DW straight in the interest of reducing DW length and its corresponding energy cost.

When edge pinning is present [see Fig. 5(a)], additional energy needs to be provided to the system in order to overcome it. Unlike the case without edge pinning where the two σ components cancel out, the two σ_E components, responsible for the DW curvature, add up and define an additional energy contribution: $2M_s H \Delta x t w = 2M_s H_{dep} \Delta x t w + 2\sigma_E \Delta x t$. This extra term also considers that the energy needed to overcome the effect of σ_E, namely, the pull back experienced by the DW due to edge pinning, is cumulative over the distance traveled by the DW (Δx). At each displacement step dx, the DW has to overcome the energy barrier imposed by σ_E; for this reason the edge pinning contribution has been proposed to scale with the total distance traveled by the DW. Within this framework, the field needed to reach the depinning condition now becomes $H - \frac{\sigma_E}{M_s w} = H_{dep}$. The edge pinning contribution is therefore evidenced in the term $H_{edge} = \frac{\sigma_E}{M_s w}$, which can be seen as an effective counter field acting on the DW due to the strong edge pinning potential.

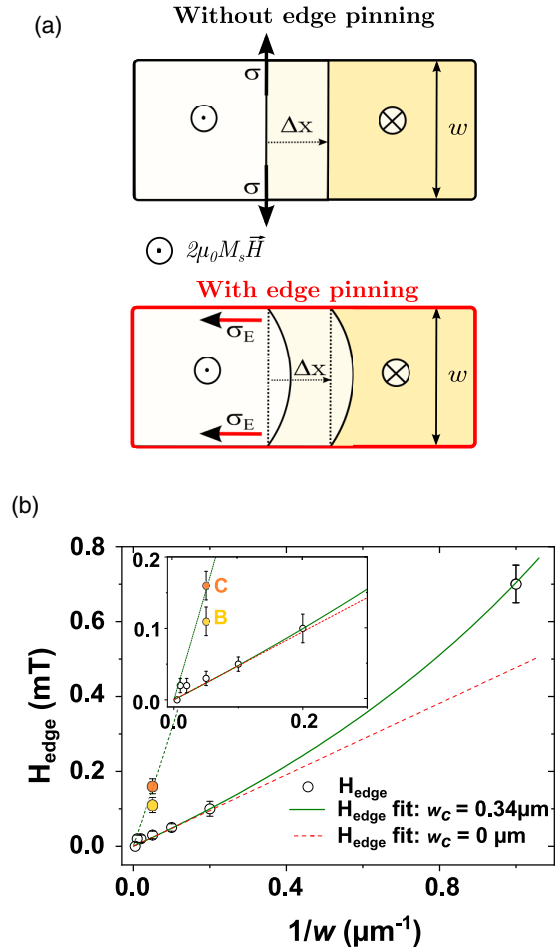

FIG. 5. (a) Graphic representation of a DW displacement Δx in the absence (top) and presence (bottom) of edge pinning. (b) H_{edge} as a function of the inverse wire width $1/w$ showing the variable width series including wire A and wires B and C. The inset shows a zoom-in of the large wire width region.

Within this simplified model, H_{edge} has a dependence on the inverse wire width. Figure 5(b) shows the dependence of H_{edge} on $1/w$, the dotted fitting line corresponds to a model considering $H_{edge} = A/w$, where w is the wire width and A the fitting parameter. This expression can describe the system at large wire widths but fails to adjust to the data for narrow wires. A more accurate description is found considering the possibility that under a certain critical wire width w_c edge pinning could be strong enough to entirely block the motion of the DW. The corresponding expression, derived from phenomenological considerations, is $H_{edge} = A/(w - w_c)$ and the fitting is plotted as a solid line in Fig. 5. Knowing that $A = \frac{\sigma_E}{M_s} = 0.46$ mT μm and that [13] $M_s = 8.7 \times 10^5$ A/m we find $\sigma_E = 4.0 \times 10^{-4}$ N/m. This value allows for a quantitative evaluation of the strength of edge pinning in wires, and it could be a useful parameter to compare between different magnetic systems and fabrication procedures. In addition, it can provide a direct link between the strength of edge pinning and the curvature of the DW. The value of σ_E can be

compared to the surface tension of the DW which is given by $\sigma = 4\sqrt{A_{ex}K_{eff}} = 11 \times 10^{-3}$ N/m, where A_{ex} is the exchange stiffness constant (2.3×10^{-11} J/m) and K_{eff} the effective anisotropy (3.4×10^{5} J/m^3) [13,15]. This gives: $\sigma/\sigma_E \approx 27$ which justifies the observation of little DW curvature in wire A [see Fig. 4(a), wire A]. On the contrary, a rough estimation of σ_E obtained for wire C [see dotted line in Fig. 5(b)] gives: $\sigma_E = 2.6 \times 10^{-3}$ N/m. As expected, enhancing the edge pinning strength compared to the DW surface tension ($\sigma/\sigma_E \approx 4$) increases the curvature of pinned DWs as shown in Fig. 4(a). Therefore, H_{edge} contains information on both edge pinning strength and DW curvature.

The good correspondence with this simple expression, derived from modeling the effects of edge pinning as a counter field, provides a framework that is unrelated to changes in the dimensionality of the system. This is compatible with the initial hypothesis stating that the wire widths studied are far from dimensions where this transformation takes place. Nevertheless, it shows that even far away from this regime, edge pinning can introduce a critical dimension below which DW motion in the framework of the creep law should not be observable. In the present case, the critical width w_c has been found to be 340 nm, and it is interesting to notice that this value coincides with the wire widths at which the effects of a 1D to 0D dimensionality change start to show in Pt/CoFe/Pt wires [10].

As mentioned earlier, the results presented here are complementary to a number of studies that have already been conducted in order to evaluate the effects of edge pinning in DW creep dynamics. DW velocity in other systems such as Pt/Co/Pt also shows a visible influence of edge pinning, mostly as an increase in H_{dep}, which is also observed in the present study (see values indicated in Fig. 1, 2, and 3). However, even in the presence of extreme artificial roughening of the wire edges the creep model can well describe the DW dynamics [3]. A good correspondence with the creep model is verified at widths significantly smaller than those showing deviations in the present study. In Pt/Co/Pt materials the creep DW dynamics, although visibly influenced by edge pinning, is largely driven by the strong pinning inside the wire which is already present in the unpatterned material. In contrast, Ta/CoFeB/MgO systems present a relatively low density of pinning centers and depinning fields [15,17]. This is also verified in the present study where only a few pinning sites are seen to pin the DW propagating inside the 200 μm wire (see Fig. 1). This is a fundamental difference with Pt/Co/Pt systems for which H_{dep} values reported can be about one order of magnitude larger than in CoFeB [2,5,9]. In this context a strong pinning potential at the wire edges in CoFeB structures has the potential to drastically change the global pinning energy landscape. A reduction of the wire width can then have a large impact already in a width range of several tens of micrometers. As the wire width decreases, the probability of finding a strong pinning site inside the wire further reduces and edge pinning can progressively become the dominant factor for creep dynamics. This does not seem to be the case in Pt/Co/Pt, where the strong intrinsic pinning defines a potential that can remain the key feature of the creep dynamics even in the presence of edge pinning.

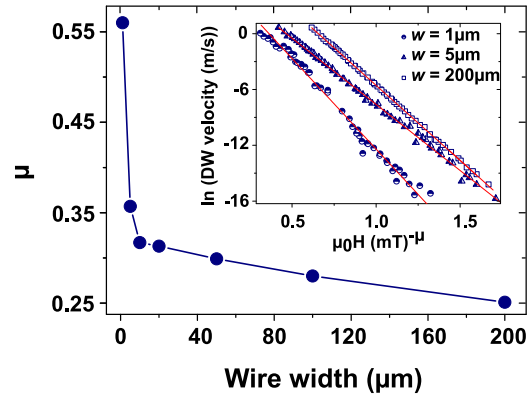

FIG. 6. Dependence of the single creep exponent μ on wire widths between 200 μm and 1 μm for the wire series A. (inset) ln(DW velocity) vs $\mu_0 H^{-\mu}$ for wire widths of 1 μm (circles, $\mu = 0.56$), 5 μm (triangles, $\mu = 0.35$), and 200 μm (squares, $\mu = 0.25$), and the respective fitting curves (solid lines).

II. ALTERNATIVE MODELS

In this section we explore the analysis of the creep model deviations by allowing variations of the creep exponent μ. In the first alternative model a single exponent is used to fit the entire velocity range, including deviations, and is seen to dramatically increase as the wire width decreases. The dependence of this variable μ exponent on the wire width is shown in Fig. 6 together with the fitting of the velocity curves for 1, 5, and 200 μm (inset). Although this stretched exponential with a variable exponent can mathematically describe the experimental data it seems inappropriate in the present case since nonuniversal exponents are retrieved as a result of the modeling. This is confirmed by the unphysical trends obtained from fitting parameters such as T_{dep}, which is found to decrease as the wire becomes narrower. This is in clear contrast with the experimental observations indicating that pinning, and therefore the depinning energy barrier, increases as the wire width decreases.

Another alternative model can be explored by thinking in terms of a pure edge pinning contribution that combines with the regular bulk creep dynamics. In this context, rescaled [18] velocity curves, presented in Fig. 7, allow us to better identify the field range in which they behave as predicted by the creep model and the point where deviations start for each individual wire with respect to a full film (200 μm wire).

In this framework, a mixed creep model could include a contribution from the pure 'bulk' creep corresponding to Eqs. (1) and (2) and taking place at the center of the wire, plus a second contribution of the same form accounting for a pure edge contribution. A simple inspection of the data points suggests that the pure bulk creep DW velocity is being reduced due to the additional contribution, therefore it can be proposed that the edge pinning contribution could be estimated by subtracting the measured DW velocity in all wires from the pure creep model expected in the absence of edge pinning (fitting line of the data obtained for a 200μ wire, the red line in Figs. 2 and 6). Figures 8(a) and 8(b) show these differences, done point by point for all wire widths and the 20 μm series, respectively. These curves are found to follow a common

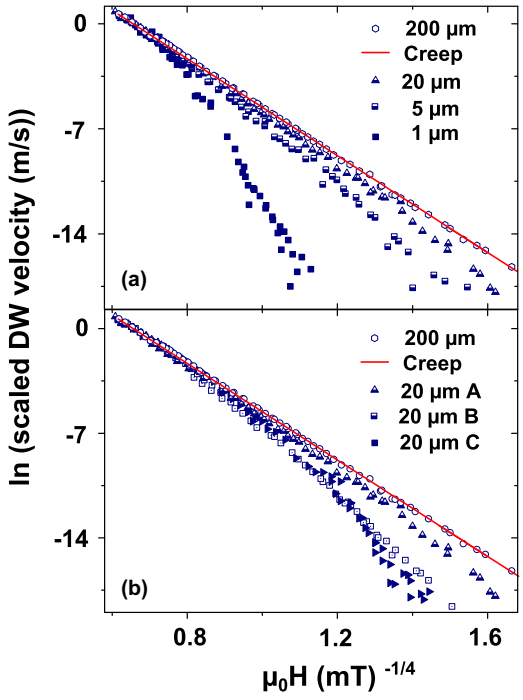

FIG. 7. Scaled ln(DW velocity) vs $\mu_0 H^{-1/4}$ for (a) all wire widths and for (b) the 20 μm wire series.

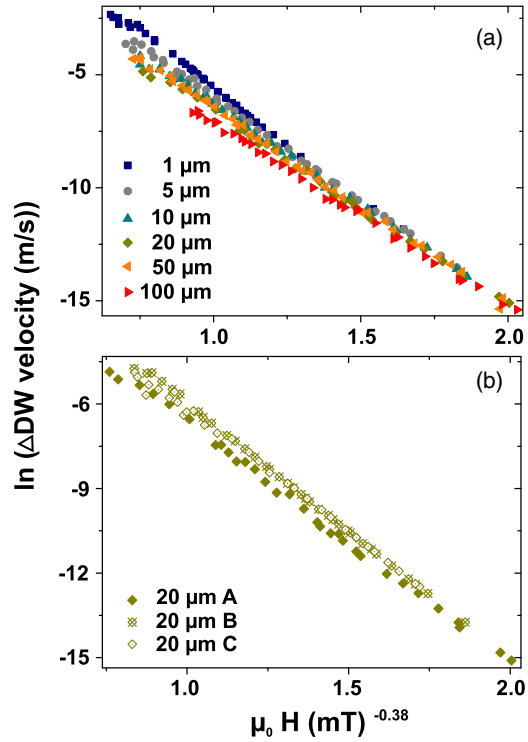

FIG. 8. DW velocity difference between the measured velocity and the pure creep model for (a) all wire widths and (b) the 20 μm wire series with respect to the pure creep model dynamics. ln(ΔDW velocity) vs $\mu_0 H^{-0.38}$ shows a linear trend.

trend and plotted as ln(ΔDW velocity) vs $\mu_0 H^{-0.38}$ present a linear dependence. The exponent of approximately 0.38 can be deduced from fitting these curves using a creeplike expression where the exponent μ is now also a fitting parameter. Therefore, from this perspective it could be assumed that an edge pinning contribution with a critical exponent close to 0.38 is at play and that its combination with the bulk pinning contribution accounts for the observed deviation from the pure bulk creep model. A fit of the velocity curves with a mixed creep model taking into account a contribution from bulk pinning with exponent $\mu = 1/4$ and an edge pinning contribution with exponent 0.38 could be done, however, there is no direct connection with a physical process justifying this mathematical treatment as there is in the case of the counter field model presented earlier. However, it is worth noting that other studies dealing with DW creep dynamics have already reported similar exponents as the one discussed here. In CoFeB/MgO and for similar wire widths (5 and 10 μm wire widths) an exponent of 0.39 is observed for creep DW motion driven by electrical currents [11]. In this case, distortions of the internal structure of the DWs under current induced DW motion are proposed as the reason behind a change in dimensionality class of the system (away from $\mu = 1/4$), leading to a change in the critical exponent. However, the significant difference between the experimentally obtained value of the critical exponent (0.39) and the theoretical value of $\mu = 1/2$ corresponding to the new dimensionality class that is discussed indicates that other factors might be at play. This same question is raised also in GaMnAs systems where DW motion under current is also proposed to fall into a universality class characterized by the critical exponent $\mu = 1/2$, and where the experimental value of 0.33 that is obtained is significantly lower [12].

In the present system a global change in universality class can be ruled out as a mechanism behind the observed deviations given the large length scales involved. The possibility of an independent process happening at the wire edges where a different dimensionality class is at play could be envisioned, however, the exponents ruling universal processes are well defined and those that could be extracted from the data in this study do not fall into that category. The alternative models presented find a dependence of the edge contribution on either a single or multiple exponents that are nonuniversal and therefore cannot be related to a physical process taking place within the framework of the creep dynamics. Nevertheless, we show that at the same time another model with a clear physical connection can very well describe the system. Finding nonuniversal exponents in the analysis of universal behavior could be an indication that the universality class is conserved and that a simpler model, not including a change in universality class, can provide an accurate description.

In conclusion, important deviations from the bulk creep DW dynamics in CoFeB/MgO have been observed due to micropatterning of the full film into wire structures. These deviations occur for larger dimensions than those where dimensionality changes can be expected. The effect is found to be related to a strong wire edge pinning potential that can progressively dominate the pinning mechanism over the intrinsic bulk potential as the wire width decreases. This scenario can be well described by modifying the bulk creep law to include the edge pinning contribution as a counter field

acting on the DW and hindering its motion. This model also shows a dependence of the counter field on the inverse of the wire width and introduces the concept of a critical width below which edge pinning could completely block DW motion. The link between this critical wire width and the length scales at which dimensionality changes can take place constitutes an interesting perspective for further investigation.

ACKNOWLEDGMENTS

We would like to thank S. Guilet and F. Bayle for assistance during sample fabrication and characterization. We gratefully acknowledge financial support from the European Union FP7 program (ITN WALL No. 608031) as well as from the French national research agency (COMAG, ELECSPIN).

[1] P. Chauve, T. Giamarchi, and P. Le Doussal, Phys. Rev. B **62**, 6241 (2000).

[2] S. Lemerle, J. Ferré, C. Chappert, V. Mathet, T. Giamarchi, P. Le Doussal, Phys. Rev. Lett. **80**, 849 (1998).

[3] F. Cayssol, D. Ravelosona, C. Chappert, J. Ferré, and J. P. Jamet, Phys. Rev. Lett. **92**, 107202 (2004).

[4] A. B. Kolton, A. Rosso, and T. Giamarchi, Phys. Rev. Lett. **94**, 047002 (2005).

[5] P. J. Metaxas, J. P. Jamet, A. Mougin, M. Cormier, J. Ferré, V. Baltz, B. Rodmacq, B. Dieny, and R. L. Stamps, Phys. Rev. Lett. **99**, 217208 (2007).

[6] G. Blatter, M. V. Fiegelman, V. B. Geshkenbien, A. I. Larkin, and V. M. Vinokur, Rev. Mod. Phys. **66**, 1125 (1994).

[7] P. Le Doussal, K. J. Wiese, S. Moulinet, and E. Rolley, Europhys. Lett. **87**, 56001 (2009).

[8] D. Bonamy, S. Santucci, and L. Ponson, Phys. Rev. Lett. **101**, 045501 (2008).

[9] V. Jeudy, A. Mougin, S. Bustingorry, W. Savero Torres, J. Gorchon, A. B. Kolton, A. Lemaitre, and J.-P. Jamet, Phys. Rev. Lett. **117**, 057201 (2016).

[10] K.-J. Kim, J.-C. Lee, S.-M. Ahn, K.-S. Lee, C.-W. Lee, Y. J. Cho, S. Seo, K.-H. Shin, S.-B. Choe, and H.-W. Lee, Nature (London) **458**, 740 (2009).

[11] S. DuttaGupta, S. Fukami, C. Zhang, H. Sato, M. Yamanouchi, F. Matsukuraand, and H. Ohno, Nat. Phys. **12**, 333 (2016).

[12] M. Yamanouchi, J. Ieda, F. Matsukura, S. E. Barnes, S. Maekawa, and H. Ohno, Science **317**, 1726 (2007).

[13] L. Herrera Diez, F. García-Sánchez, J.-P. Adam, T. Devolder, S. Eimer, M. S. El Hadri, A. Lamperti, R. Mantovan, B. Ocker, and D. Ravelosona, Appl. Phys. Lett. **107**, 032401 (2015).

[14] R. D. Pardo, W. S. Torres, A. B. Kolton, S. Bustingorry, and V. Jeudy, Phys. Rev. B **95**, 184434 (2017).

[15] C. Burrowes, N. Vernier, J.-P. Adam, L. Herrera Diez, K. Garcia, I. Barisic, G. Agnus, S. Eimer, J.-V. Kim, T. Devolder, A. Lamperti, R. Mantovan, B. Ockert, E. E. Fullerton, and D. Ravelosona, Appl. Phys. Lett. **103**, 182401 (2013).

[16] R. L. Novak, P. J. Metaxas, J.-P. Jamet, R. Weil, J. Ferré, A. Mougin, S. Rohart, R. L. Stamps, P.-J. Zermatten, G. Gaudin, V. Baltz, and B. Rodmacq, J. Phys. D: Appl. Phys. **48**, 235004 (2015).

[17] J.-P. Tetienne, T. Hingant, J.-V. Kim, L. Herrera Diez, J.-P. Adam, K. Garcia, J.-F. Roch, S. Rohart, A. Thiaville, D. Ravelosona, and V. Jacques, Science **344**, 1366 (2014).

[18] DW velocity differences at high fields between different wires have been eliminated. This was carried out by adding a vertical offset to all DW velocity curves to clearly see the field range in which they collapse with the original 200 μm wire curve.